Simulation of SIS model over networks

Virginia Nicosia, Gabriele Villa

December 2025

1 Introduction

Epidemic spreading processes on networks have been widely studied to understand how the underlying topology affects the persistence and extinction of diseases; among the simplest models capturing reinfection mechanisms there is the SIS (Susceptible Infected Susceptible) model, in which nodes can alternate indefinitely between healthy and infected states.

A key theoretical result for SIS dynamics on networks is the existence of an epidemic threshold, which depends on the spectral properties of the adjacency matrix. In particular, mean-field theory predicts that the critical transmission rate is inversely proportional to the leading eigenvalue of the adjacency matrix.

In this work, we investigate how different network topologies influence SIS dynamics, both above and below the epidemic threshold. We consider several canonical network models, including random, small-world, scale-free and highly structured graphs and compare their dynamical behavior through numerical simulations.

2 Results

2.1 Spectral properties and thresholds

Table 2.1 reports the leading eigenvalue λ_1 of the adjacency matrix for each network and the corresponding SIS epidemic threshold $\beta_c = \gamma/\lambda_1$. Highly connected and heterogeneous networks, such as the complete graph and the star, exhibit very large spectral radius and consequently extremely small epidemic thresholds, while sparse and structured networks such as trees and lattices display significantly smaller values of λ_1, leading to much higher critical transmission rates. Erdős–Rényi and Watts–Strogatz networks show similar spectral properties and thresholds, reflecting their comparable average connectivity.

Table 1: Leading eigenvalue and SIS epidemic threshold

Network	Lambda1	Beta_c
ER	10.9756	0.0364
BA	13.1815	0.0303
WS	10.2173	0.0391
Complete	999.0000	0.0004
Tree	2.7130	0.1474
Star	31.6070	0.0127
Lattice	3.9813	0.1005

2.2 SIS dynamics far above the epidemic threshold

Figure 1 shows the temporal evolution of the fraction of infected nodes for a fixed transmission rate $\beta = 0.6$, which lies well above the epidemic threshold for all the considered networks. The value $\beta = 0.6$ was chosen to place the system deep in the supercritical regime for all networks, allowing a clear comparison of endemic states across different topologies. In this regime, the infection rapidly spreads and reaches an endemic steady state.

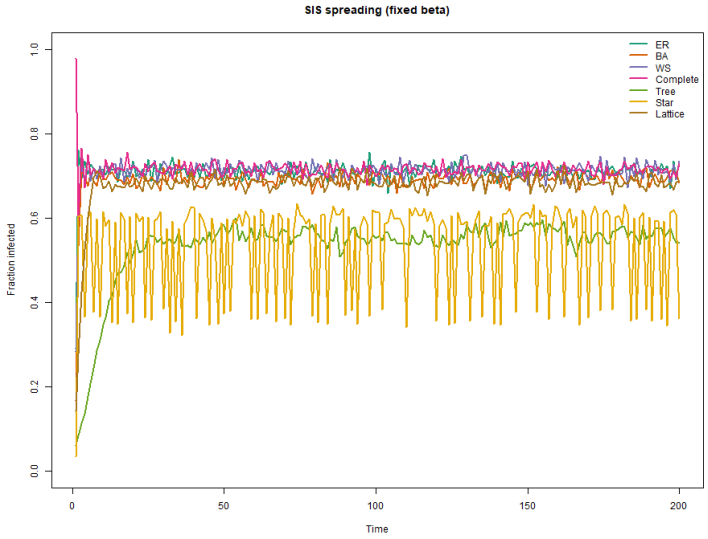

Figure 1: Time evolution of the fraction of infected nodes for the SIS model with fixed transmission rate $\beta = 0.6$ on different network topologies.

2.3 Dynamics close to the epidemic threshold

To investigate the transition between extinction and persistence, SIS simulations were performed for transmission rates slightly below and above the epidemic threshold β_c for each network. Figures 2–8 illustrate the resulting dynamics.

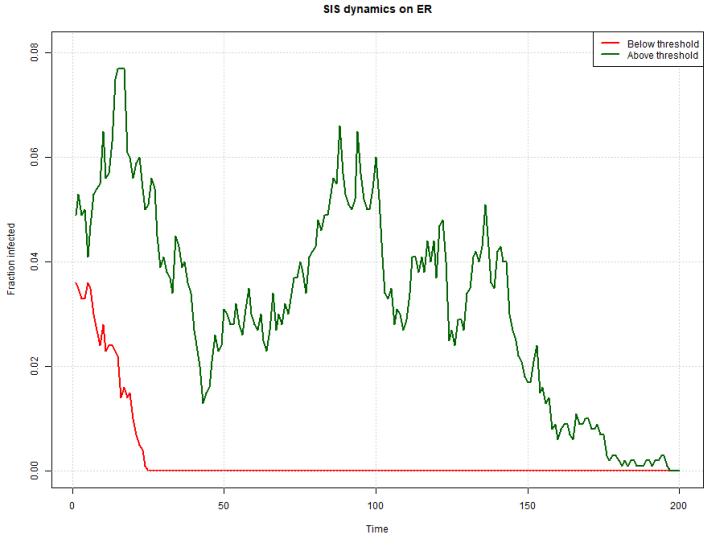

Figure 2: SIS dynamics on an Erdős–Rényi network for transmission rates slightly below and above the epidemic threshold β_c.

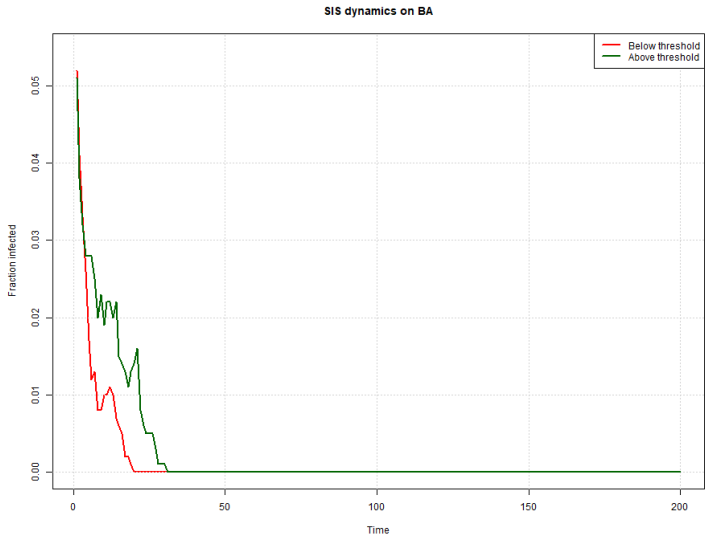

Figure 3: SIS dynamics on a Barabási–Albert network for transmission rates slightly below and above the epidemic threshold β_c.

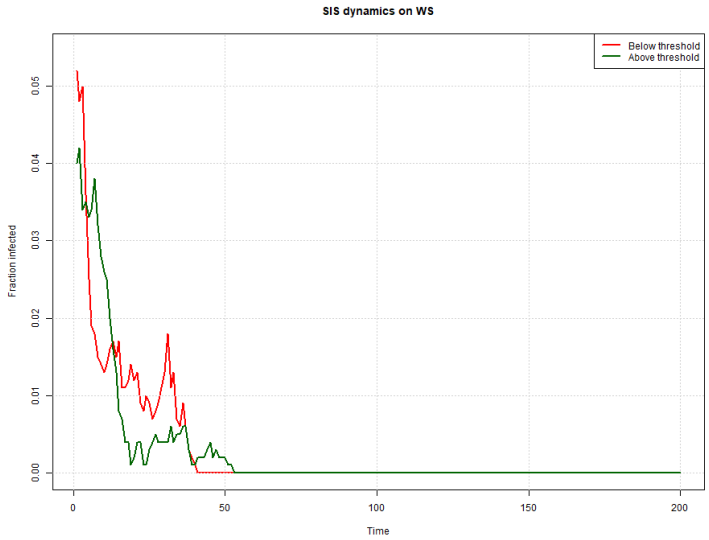

Figure 4: SIS dynamics on a Watts–Strogatz network for transmission rates slightly below and above the epidemic threshold β_c.

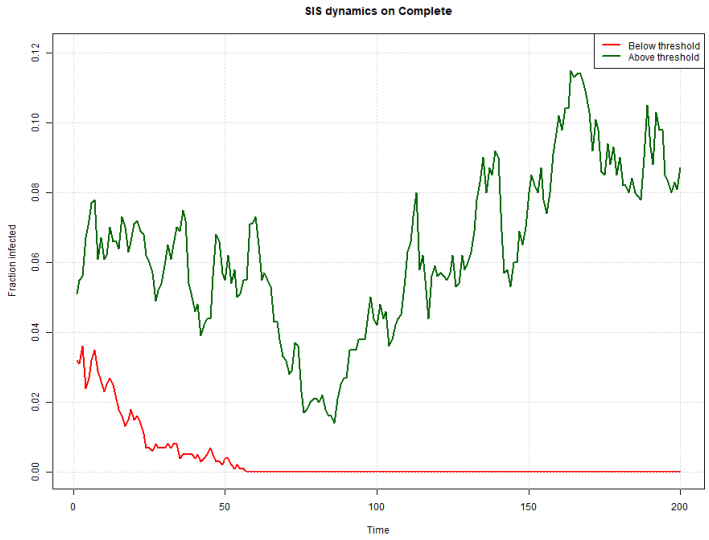

Figure 5: SIS dynamics on a complete graph for transmission rates slightly below and above the epidemic threshold β_c.

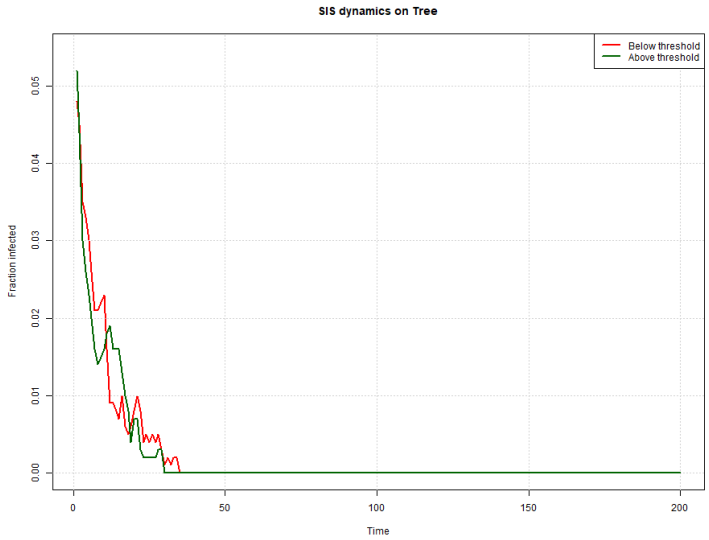

Figure 6: SIS dynamics on a tree network for transmission rates slightly below and above the epidemic threshold β_c.

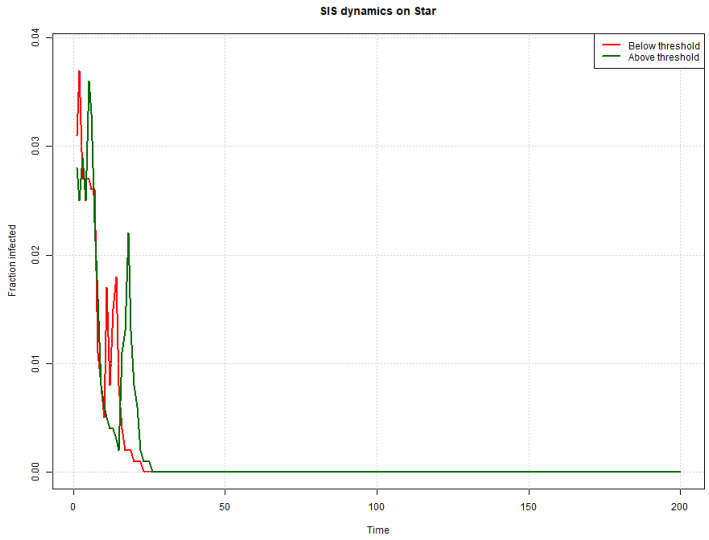

Figure 7: SIS dynamics on a star network for transmission rates slightly below and above the epidemic threshold β_c.

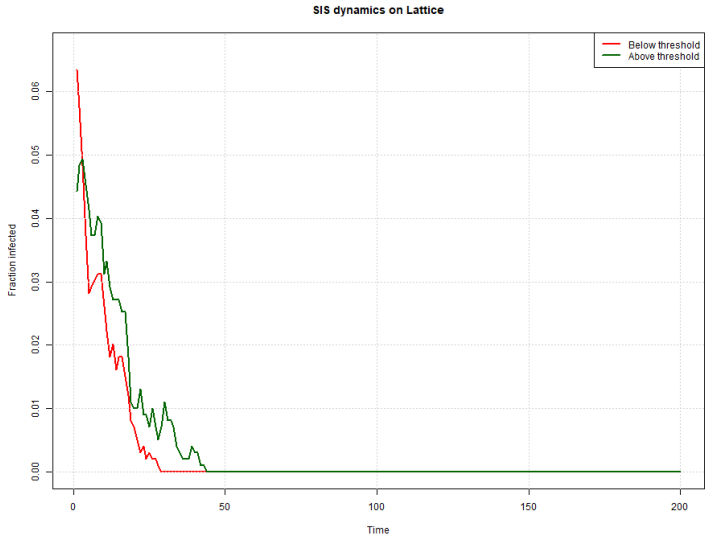

Figure 8: SIS dynamics on a two dimensional lattice for transmission rates slightly below and above the epidemic threshold β_c.

3 Discussion of Results (Task 1)

The temporal evolution of the fraction of infected nodes for the seven considered network topologies is shown in Figure 1. The simulation was performed with a fixed set of parameters ($\beta = 0.6, \gamma = 0.4, p_0 = 0.05$) across all networks to allow for a direct comparison of the topological effects on the spreading dynamics.

3.1 Epidemic Susceptibility and Network Topology

Based on the simulation results, the Complete graph (pink line) is the most prone to the epidemic, exhibiting the fastest initial growth rate and saturating the network. This behavior is expected, as the fully connected structure maximizes the spreading potential.

The Barabási-Albert (BA) network (orange line) also demonstrates high susceptibility. Consistent with scale-free topologies, it shows a rapid initial rise in infection. This is driven by the presence of high-degree hubs: once infected, these nodes act as "superspreaders", transmitting the disease to a large number of neighbors simultaneously.

Despite their structural differences, the Erdős–Rényi (ER), Watts-Strogatz (WS) and Lattice networks display stationary infection levels very similar to the Complete and BA graphs. This indicates that, when the infection rate is sufficiently above the threshold, the SIS dynamics on these connected networks become weakly dependent on detailed topological features, driven mostly by the average degree.

In contrast, the Star graph (yellow line) shows a highly volatile behavior. While it reaches a significant infection fraction, it exhibits large oscillations. This variance is characteristic of star topologies where the state of the central hub dictates the overall prevalence; if the hub recovers, the infection level drops sharply until the hub is reinfected.

Finally, sparse networks such as the Tree, exhibit lower endemic prevalence and slower growth rates, reflecting its reduced connectivity and longer average path lengths, which hinder the rapid propagation of the virus.

3.2 Consistency with Spectral Graph Theory

To verify the theoretical consistency of these results, we checked the leading eigenvalue (λ_1) of the adjacency matrix for each network. Theory predicts the epidemic threshold to be $\tau = \frac{\gamma}{\lambda_1}$ [Chakrabarti et al., 2008]. Table 2.1 summarizes the computed eigenvalues.

The simulation results are fully consistent with the spectral properties:

- **High λ_1 (Highest Susceptibility):** The Complete graph ($\lambda_1 = 999$) and the Star graph ($\lambda_1 \approx 31.6$) have the largest spectral radii, corresponding to the lowest theoretical thresholds.
- **Moderate λ_1:** The Barabási-Albert ($\lambda_1 \approx 13.18$), Erdős–Rényi ($\lambda_1 \approx 10.98$), and Watts–Strogatz ($\lambda_1 \approx 10.22$) networks possess comparable spectral radii. This proximity in values explains why these three networks eventually settle at very similar steady-state infection levels in Figure 1.
- **Low λ_1 (Lowest Susceptibility):** The Tree ($\lambda_1 \approx 2.71$) and Lattice ($\lambda_1 \approx 3.98$) have the lowest eigenvalues. Consequently, they have the highest epidemic thresholds, requiring a much stronger transmission rate to sustain the disease. This is reflected in the plot in the case of Tree, where this network shows the lowest prevalence levels.

In conclusion, the simulation confirms that networks with larger leading eigenvalues are more prone to epidemics, exhibiting faster spreading rates and higher prevalence levels, as predicted by the SIS model theory.

4 Discussion of Results (Task 2)

In this task, we verified the epidemic threshold predictions by simulating the spread of the disease with infection probabilities slightly below ($\beta_{below} = 0.9 \cdot \beta_c$) and slightly above ($\beta_{above} = 1.1 \cdot \beta_c$) the theoretical critical point calculated in Task 1. The results for the different network topologies are illustrated in the generated figures.

4.1 Threshold Sensitivity and Phase Transition

The simulation results provide a qualitative confirmation of the spectral threshold theory, although the distinction between the two regimes is heavily influenced by stochastic effects in finite networks.

4.1.1 Clear Separation: The Complete Graph

The most robust validation of the theory is observed in the Complete network. As shown in the plot, the sub-threshold simulation (red line) rapidly decays to zero, confirming the extinction of the disease. Conversely, the supra-threshold simulation (green line) successfully establishes a persistent endemic state, fluctuating around a constant prevalence. This confirms that for dense networks, β_c acts as a sharp boundary.

4.1.2 Delayed Extinction: ER

For the Erdős-Rényi (ER) network, the threshold effect manifests primarily as a difference in survival time. While the sub-threshold dynamics (red lines) die out relatively quickly (e.g., $t < 30$ for ER), the supra-threshold cases (green lines) persist significantly longer and reach higher infection peaks before eventual extinction. This indicates that crossing the threshold triggers a change in the virus's ability to propagate, even if it does not guarantee permanent survival in a single run.

4.2 Finite-Size Effects and Stochastic Extinction

In the remaining networks (Lattice, Tree, Star, BA and WS), we observe that the disease eventually dies out in both regimes (both red and green lines go to zero). However, the qualitative difference remains visible: the green lines consistently exhibit higher peaks or slower decay than the red lines.

This observed extinction above the threshold can be explained by two factors:

1. Proximity to the Threshold: We simulated at $1.1 \cdot \beta_c$, which is only marginally above the critical point. In finite-size systems ($N = 1000$), the epidemic is fragile near the transition. Random fluctuations (stochastic noise) can drive the number of infected nodes to zero, causing an accidental extinction known as finite-size stochastic die-out.

2. Topological Constraints: In networks like the Tree or Lattice, the lack of redundant paths makes the virus vulnerable to local extinctions, preventing the global endemic state from stabilizing within the observed time window.

4.3 Consistency with Theory

To answer the core question: Are the simulation results consistent with the theory?

Yes, the results are largely consistent. In all cases, the epidemic prevalence for $\beta > \beta_c$ is strictly higher (in terms of peak or duration) than for $\beta < \beta_c$. The theoretical value β_c successfully identifies the region where the system undergoes a dynamical change. The lack of permanent endemicity in the supra-threshold cases is an expected artifact of simulating finite networks close to the critical point, rather than a failure of the spectral graph theory itself.

5 Methods

5.1 Network construction

All simulations are performed on undirected, unweighted networks of fixed size $n = 1000$. Seven different network topologies are considered in order to capture a wide range of structural properties: Erdős–Rényi random graphs generated with link probability $p = 0.01$, Barabási–Albert scale-free networks constructed via preferential attachment with $m = 3$ edges added per node, Watts–Strogatz small-world networks with neighborhood size 5 and rewiring probability 0.1, complete graph, tree graph, star graph and a two-dimensional lattice with nearest-neighbor connectivity. All networks are treated as static throughout the simulations.

5.2 SIS epidemic dynamics

We study a discrete-time Susceptible–Infected–Susceptible (SIS) process. Each node can be in one of two states: susceptible or infected. At each time step, infected nodes recover independently with probability $\gamma = 0.4$ and immediately become susceptible again; susceptible nodes can become infected through contact with infected neighbors. Let $k_i(t)$ denote the number of infected neighbors of node i at time t, the probability that a susceptible node becomes infected during a single time step is given by

$$p_i(t) = 1 - (1 - \beta)^{k_i(t)}$$

which corresponds to an approximation in which infection attempts from different neighbors are treated as independent. This formulation allows efficient simulation even for large networks.

The state of the system at time t is represented by a binary vector $\mathbf{x}(t)$, where $\mathbf{x}_i(t) = 1$ if node i is infected and $\mathbf{x}_i(t) = 0$ otherwise. Simulations are initialized by infecting each node independently with probability $p_0 = 0.05$ and the process is iterated for a fixed time horizon of $T_{\max} = 200$ time steps.

The primary observable is the fraction of infected nodes,

$$\rho(t) = \frac{1}{n} \sum_{i=1}^{n} x_i(t),$$

which is recorded at each time step.

5.3 Numerical implementation

The SIS dynamics is implemented using matrix-based operations to ensure computational efficiency; for each network, the adjacency matrix is stored in sparse format. At each time step, the vector of infected neighbors is computed as the matrix–vector product between the adjacency matrix and the infection state vector. Infection probabilities are bounded to ensure numerical stability.

All simulations are stochastic and, to ensure reproducibility, the random number generator is initialized with a fixed seed.

5.4 Spectral analysis and epidemic threshold

For each network, we compute the leading eigenvalue λ_1 of the adjacency matrix using a sparse eigensolver. The epidemic threshold is then estimated according to the heterogeneous mean-field prediction

$$\beta_c = \frac{\gamma}{\lambda_1}.$$

this threshold separates regimes in which the infection dies out from those in which it can persist endemically.

To investigate the behavior near the threshold, simulations are performed for transmission rates slightly below and above β_c, specifically $\beta = 0.9\beta_c$ and $\beta = 1.1\beta_c$; this allows a direct comparison between subcritical and supercritical regimes for each network topology.